TECHNICAL REPORT SL-82-10

AN ELASTIC-VISCOPLASTIC CONSTITUTIVE MODEL FOR EARTH MATERIALS

by

George Y. Baladi and Behzad Rohani

Structures Laboratory
U. S. Army Engineer Waterways Experiment Station
P. O. Box 631, Vicksburg, Miss. 39180

December 1982
Final Report

Prepared for Office, Chief of Engineers, U. S. Army
Washington, D. C. 20314

Under Project 4A161102AT22, Task BO, Work Unit 005

Destroy this report when no longer needed. Do not return it to the originator.

The findings in this report are not to be construed as an official Department of the Army position unless so designated by other authorized documents.

The contents of this report are not to be used for advertising, publication, or promotional purposes. Citation of trade names does not constitute an official endorsement or approval of the use of such commercial products.

Unclassified

SECURITY CLASSIFICATION OF THIS PAGE (When Data Entered)

REPORT DOCUMENTATION PAGE		READ INSTRUCTIONS BEFORE COMPLETING FORM
1. REPORT NUMBER Technical Report SL-82-10	2. GOVT ACCESSION NO. AD-A123 393	3. RECIPIENT'S CATALOG NUMBER
4. TITLE (and Subtitle) AN ELASTIC-VISCOPLASTIC CONSTITUTIVE MODEL FOR EARTH MATERIALS		5. TYPE OF REPORT & PERIOD COVERED Final report 6. PERFORMING ORG. REPORT NUMBER
7. AUTHOR(s) George Y. Baladi and Behzad Rohani		8. CONTRACT OR GRANT NUMBER(s)
9. PERFORMING ORGANIZATION NAME AND ADDRESS U. S. Army Engineer Waterways Experiment Station Structures Laboratory P. O. Box 631, Vicksburg, Miss. 39180		10. PROGRAM ELEMENT, PROJECT, TASK AREA & WORK UNIT NUMBERS Project 4A161102AT22 Task B0, Work Unit 005
11. CONTROLLING OFFICE NAME AND ADDRESS Office, Chief of Engineers, U. S. Army Washington, D. C. 20314		12. REPORT DATE December 1982 13. NUMBER OF PAGES 34
14. MONITORING AGENCY NAME & ADDRESS(if different from Controlling Office)		15. SECURITY CLASS. (of this report) Unclassified 15a. DECLASSIFICATION/DOWNGRADING SCHEDULE

16. DISTRIBUTION STATEMENT (of this Report)

Approved for public release; distribution unlimited.

17. DISTRIBUTION STATEMENT (of the abstract entered in Block 20, if different from Report)

18. SUPPLEMENTARY NOTES

Available from National Technical Information Service, 5285 Port Royal Road, Springfield, Va. 22151.

19. KEY WORDS (Continue on reverse side if necessary and identify by block number)

Elastic-viscoplastic constitutive relationship
Rate-dependent material properties
Soil constitutive models
Stress-strain relations

20. ABSTRACT (Continue on reverse side if necessary and identify by block number)

It has long been recognized that the stress-strain-strength properties of most geological materials under high-intensity dynamic loading conditions differ considerably from those related to relatively low-intensity static loadings. Thus realistic solutions to soil dynamic boundary-value problems require the use of constitutive models that can account for the dependency of the stress-strain-strength properties of earth materials to the various rates of loading or deformation being applied.

(Continued)

DD FORM 1 JAN 73 1473 EDITION OF 1 NOV 65 IS OBSOLETE

Unclassified

SECURITY CLASSIFICATION OF THIS PAGE (When Data Entered)

20. ABSTRACT (Continued)

This report describes the development of a three-dimensional elastic-viscoplastic work-hardening constitutive relationship for earth materials. The constitutive relationship is capable of reproducing the hysteretic behavior of the material under both hydrostatic and deviatoric states of stress; it also accounts for shear-induced volume change and the effect of superimposed hydrostatic stress on shearing response. The capability of the constitutive relationship for simulating the time-dependent response of earth materials is examined; an example fit for a clayey sand is given based on static laboratory triaxial shear and static and dynamic uniaxial strain test results.

PREFACE

This investigation was conducted for the Office, Chief of Engineers, U. S. Army, by personnel of the Geomechanics Division (GD), Structures Laboratory (SL), U. S. Army Engineer Waterways Experiment Station (WES), as a part of Project 4A161102AT22, Task B0, Work Unit 005, "Constitutive Properties for Natural Earth and Man-Made Materials." This report was prepared by Drs. George Y. Baladi and Behzad Rohani during the period January-July 1982 under the general direction of Mr. Bryant Mather, Chief, SL, and Dr. J. G. Jackson, Jr., Chief, GD. The report was typed by Mrs. Bobbie B. Morrow.

COL Tilford C. Creel, CE, was Commander and Director of WES during this investigation. Mr. F. R. Brown was Technical Director.

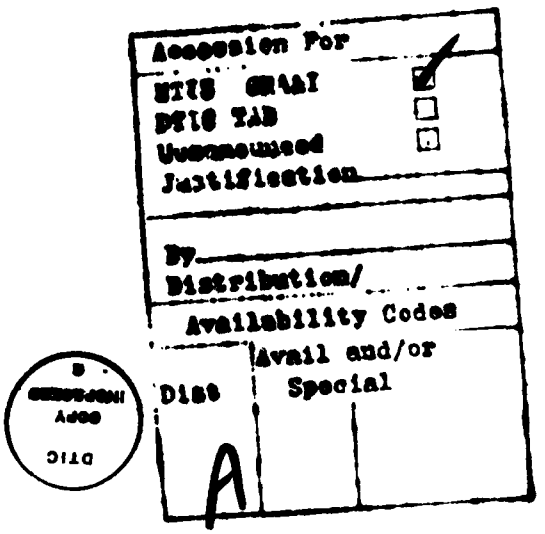

CONTENTS

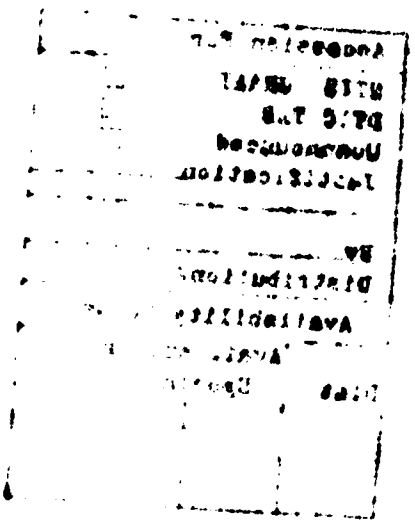

CONVERSION FACTORS, METRIC (SI) U. S. CUSTOMARY UNITS OF MEASUREMENT

Units of measurement used in this report can be converted as follows:

Multiply	By	To Obtain
centimetres	0.3937007	inches
centimetres per millisecond	0.3937007	inches per millisecond
grams per cubic centimetre	62.42797	pounds (mass) per cubic foot
metres	3.280839	feet
metres per millisecond	3.280839	feet per millisecond
millimetres	0.03937007	inches
megapascals	145.0377439	pounds per square inch

AN ELASTIC-VISCOPLASTIC CONSTITUTIVE MODEL FOR EARTH MATERIALS

PART I: INTRODUCTION

1. The mechanical response of most earth materials subjected to high-intensity dynamic loadings, such as those produced by large explosive detonations and impact of high-velocity projectiles, differs considerably from what is usually observed under relatively low-intensity static loadings (very slow rates of deformation). In order to obtain realistic solutions for dynamic problems, a constitutive model should be used that can account for the dependency of the stress-strain-strength properties of earth materials on the various rates of loading or deformation being applied. In addition, the constitutive model should account for other pertinent features of the stress-strain properties of earth materials observed under both dynamic and static loading conditions, such as (a) the dependency of the shearing strength of the material on hydrostatic stress, (b) shear-induced volume change, and (c) permanent strain during a load-unload cycle of deformation (for both deviatoric and hydrostatic loading conditions).

2. Incremental elastic-plastic constitutive models have been used successfully to simulate the stress-strain properties of soil (Baladi and Rohani, 1979; Baladi, 1977; and Sandler, DiMaggio, and Baladi, 1976). It is therefore logical to adopt a physically realistic incremental elastic-plastic constitutive model for earth materials and introduce rate dependency in such a model. Generally, two different types of rate-dependent models can be constructed in this manner: viscoelastic-plastic models in which both the elastic and the plastic responses of the material are rate-sensitive; and elastic-viscoplastic models in which the plastic portion of the model is rate-dependent and the elastic portion is rate-independent. As pointed out by Perzyna (1966), the viscoelastic-plastic models are mathematically very complicated and are not suitable for solving practical engineering problems. The elastic-viscoplastic models, because of their mathematical simplicity

(relative to viscoelastic-plastic models) and their similarities with the inviscid theory of plasticity, are more appropriate for practical engineering application (Perzyna, 1966; Swift, 1975). Also, viscous effects appear to be more evident in the plastic range for most soils. Thus, it is reasonable to adopt an elastic-viscoplastic type constitutive relationship to model the rate-dependent response of earth materials. Application of this type of model for describing the rate-dependent response of rocks is discussed by DiMaggio and Sandler (1971).

3. This report describes the fundamental basis of elastic-viscoplastic constitutive relationships and the development of a specific model of this type for earth materials. To demonstrate the application of the model, its behavior under cylindrical states of stress is examined and correlated with experimental data for a clayey sand.

PART II: FUNDAMENTAL BASIS OF ELASTIC-VISCOPLASTIC CONSTITUTIVE RELATIONSHIPS

4. The basic premise of elastic-plastic constitutive relationships is the assumption that certain materials are capable of undergoing small plastic (permanent) as well as elastic (recoverable) strains at each loading increment.* In the case of elastic-viscoplastic materials, it is further assumed that the behavior of the material in the plastic region is rate-dependent. Mathematically, the total strain rate is assumed to be the sum of the elastic components and the viscoplastic components, i.e.,

$$\frac{d\varepsilon_{ij}}{dt} = \frac{d\varepsilon^{E}_{ij}}{dt} + \frac{d\varepsilon^{vp}_{ij}}{dt} \tag{1}$$

where

$\frac{d\varepsilon_{ij}}{dt}$ = total components of the strain rate tensor

$\frac{d\varepsilon^{E}_{ij}}{dt}$ = components of the elastic strain rate tensor

$\frac{d\varepsilon^{vp}_{ij}}{dt}$ = components of the viscoplastic strain rate tensor

Elastic Strain Rate Tensor

5. Within the elastic range, the behavior of the material can be described by an elastic constitutive relation of the type

$$\frac{d\varepsilon^{E}_{ij}}{dt} = C_{ijk\ell}\,(\sigma_{mn})\,\frac{d\sigma_{k\ell}}{dt} \tag{2}$$

---

* In this paper, compression is considered positive.

where

$C_{ijk\ell}$ = material response function

$\frac{d\sigma_{k\ell}}{dt}$ = components of stress rate tensor

σ_{mn} = components of stress tensor

For isotropic compressible elastic materials, the simplest form of Equation 2 is

$$\frac{d\varepsilon^{E}_{ij}}{dt} = \frac{1}{9K}\frac{dJ_1}{dt}\delta_{ij} + \frac{1}{2G}\frac{dS_{ij}}{dt} \tag{3}$$

where

$J_1 = \sigma_{mm}$ = first invariant of stress tensor

$S_{ij} = \sigma_{ij} - \frac{J_1}{3}\delta_{ij}$ = stress deviation tensor

K = elastic bulk modulus

G = elastic shear modulus

δ_{ij} = Kronecker delta = $\begin{cases} 1 & i = j \\ 0 & i \neq j \end{cases}$

6. The bulk and shear moduli can be expressed as functions of the invariants of the stress tensor. However, in order not to generate energy or hysteresis within the elastic range, the elastic response must be path-independent. This condition can be met if and only if the bulk modulus is a function of the first invariant of the stress tensor and the shear modulus is a function of the second invariant of the stress deviation tensor (Sandler, DiMaggio, and Baladi, 1976). Thus,

$$K = K(J_1); \quad G = G(J_2') \tag{4}$$

where

$J_2' = \frac{1}{2} S_{ij} S_{ij}$ = the second invariant of the stress deviation tensor

Viscoplastic Strain Rate Tensor

7. The behavior of the material in the plastic range is assumed to be rate-sensitive. As indicated by Perzyna (1966), the viscoplastic component of the strain rate tensor can be expressed as an arbitrary function of the "excess stress" above the initial yield condition which is called the static yield criterion. The static yield criterion should satisfy all the known conditions of the inviscid theory of plasticity (Drucker, 1956). In general, the static yield surface may be expressed as

$$f_s(\sigma_{ij}, \kappa) = 0 \tag{5}$$

For isotropic materials the static yield surface may be expressed, for example, as

$$f_s(J_1, \sqrt{J_2'}, \kappa) = 0 \tag{6}$$

where κ is a hardening parameter and generally is a function of the viscoplastic (or plastic) deformation. The static yield surface (Equation 6) may expand or contract as κ increases or decreases, respectively (Figure 1).

8. Since the viscoplastic strain rate is an arbitrary function of the excess stress above the static yield criterion, the "dynamic yield surface" can be defined as

$$f_d(J_1, \sqrt{J_2'}, \kappa, \beta) = \frac{f_s(J_1, \sqrt{J_2'}, \kappa) - \beta}{B} = 0 \tag{7}$$

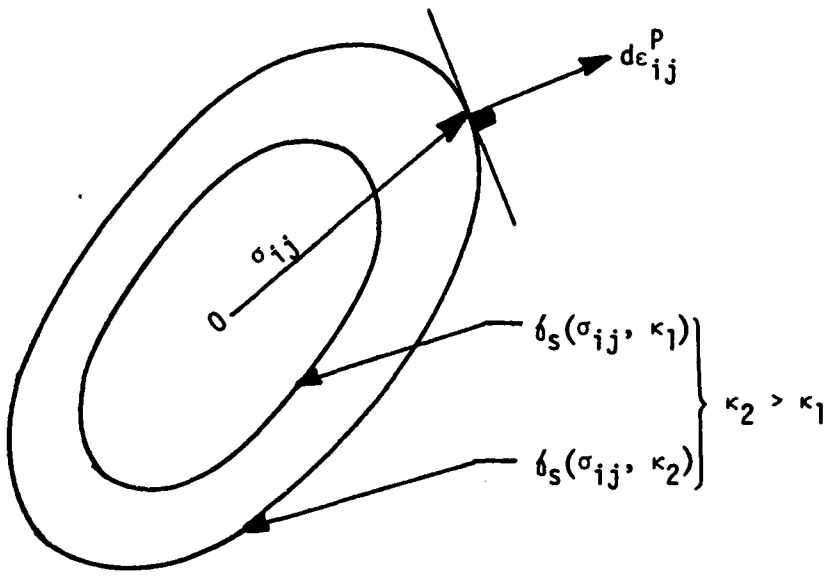

Figure 1. Work-hardening loading surface and plastic strain increment vector

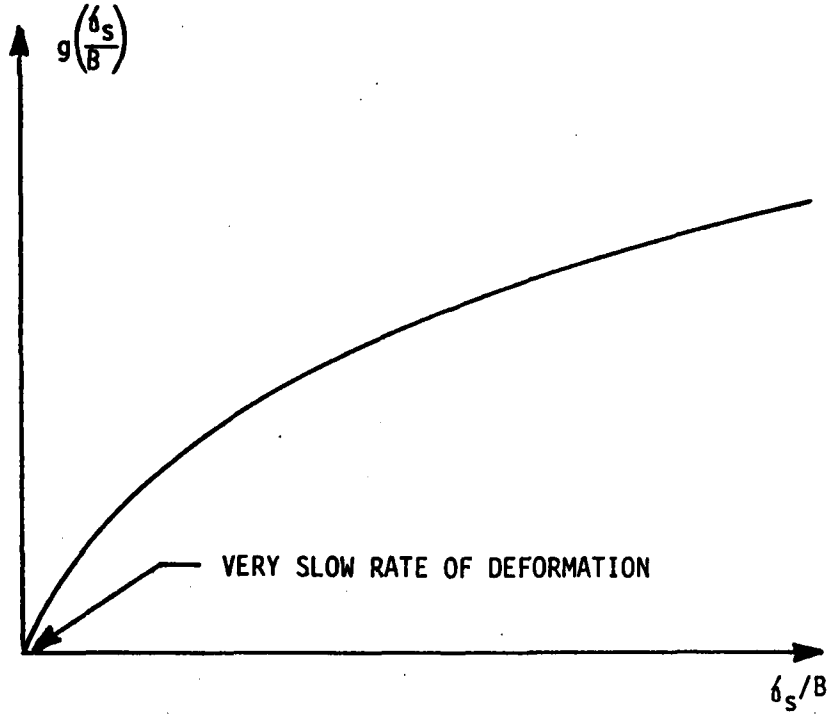

Figure 2. Typical behavior of the function $g(f_s/B)$ for viscoplastic materials

and the flow rule for work-hardening and rate-sensitive plastic materials may be written as

$$\frac{d\varepsilon_{ij}^{vp}}{dt} = \begin{cases} \gamma g\left(\frac{\sigma_s}{B}\right) \frac{\partial \sigma_s}{\partial \sigma_{ij}} & \text{if } \sigma_s > 0 \\ 0 & \text{if } \sigma_s \leq 0 \end{cases} \tag{8}$$

The parameter β/B in Equation 7 is dimensionless and defines the rate of expansion of the yield surface. (B is a scaling factor which has the dimension of stress; it is introduced in Equation 7 to make σ_d dimensionless.) The function $g(\sigma_s/B)$ in Equation 8 is a dimensionless function which may be determined from the results of dynamic property tests for the material of interest (Figure 2). The parameter γ in Equation 8 is a viscosity parameter associated with the viscoplastic response of the material and has the dimension of $(\text{time})^{-1}$. It should be pointed out that for very slow rates of deformation, β and $g(\sigma_s/B)$ approach zero. Hence, σ_d and σ_s become identical and the viscoplastic flow rule (Equation 8) reduces to its inviscid counterpart.

9. The viscoplastic stress-strain relation can be expressed in terms of the hydrostatic and deviatoric components of strain. Applying the chain rule of differentiation to the right-hand side of Equation 8 yields

$$\frac{d\varepsilon_{ij}^{vp}}{dt} = \gamma g\left(\frac{\sigma_s}{B}\right)\left[\frac{\partial \sigma_s}{\partial J_1}\delta_{ij} + \frac{1}{2\sqrt{J_2'}}\frac{\partial \sigma_s}{\partial \sqrt{J_2'}} S_{ij}\right] \tag{9}$$

Multiplying both sides of Equation 9 by δ_{ij} gives

$$\frac{d\varepsilon_{kk}^{vp}}{dt} = 3\gamma g\left(\frac{\sigma_s}{B}\right)\frac{\partial \sigma_s}{\partial J_1} \tag{10}$$

The deviatoric component of the viscoplastic strain rate tensor de_{ij}^{vp}/dt can be written as

$$\frac{de_{ij}^{vp}}{dt} = \frac{d\varepsilon_{ij}^{vp}}{dt} - \frac{1}{3}\frac{d\varepsilon_{kk}^{vp}}{dt}\delta_{ij} \tag{11}$$

Substitution of Equations 9 and 10 into Equation 11 yields

$$\frac{de_{ij}^{vp}}{dt} = \gamma g\left(\frac{\sigma_s}{B}\right)\frac{S_{ij}}{2\sqrt{J_2'}}\frac{\partial \sigma_s}{\partial \sqrt{J_2'}} \tag{12}$$

The associated flow rule is satisfied when Equations 10 and 12 are used with Equation 7; this shows that the vector $d\varepsilon_{ij}^{vp}/dt$ in the $(J_1, \sqrt{J_2'})$ space is always normal to the surface $\sigma_s(J_1, \sqrt{J_2'}, \kappa) = \beta$ (Figure 3). Squaring both sides of Equation 9 gives

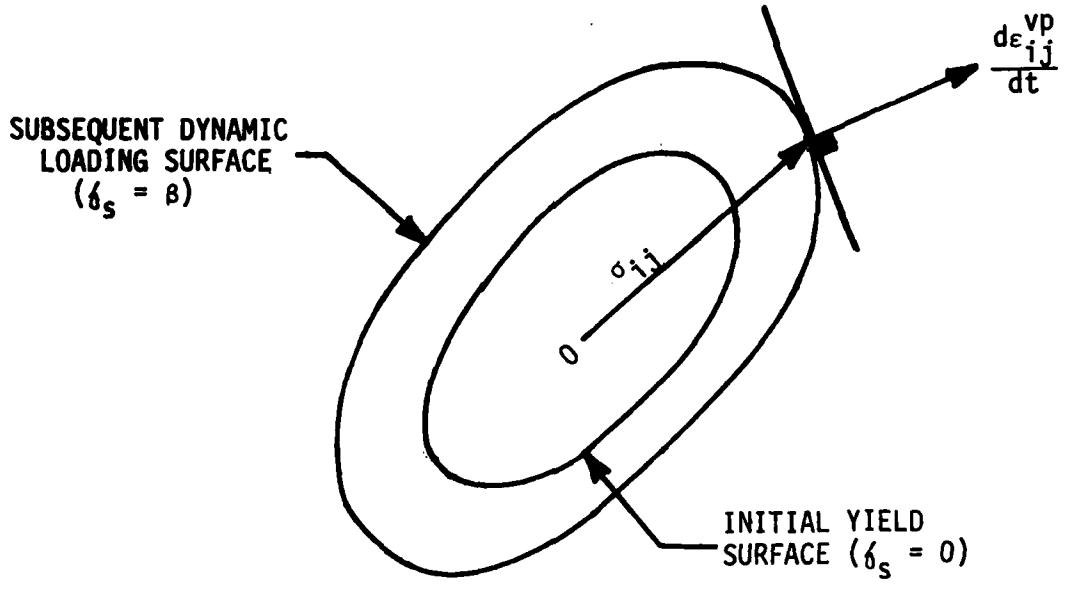

Figure 3. Dynamic loading surface and strain rate vector

$$\gamma g\left(\frac{\sigma_s}{B}\right) = \left[\frac{\frac{d\varepsilon_{ij}^{vp}}{dt}\frac{d\varepsilon_{ij}^{vp}}{dt}}{3\left(\frac{\partial \sigma_s}{\partial J_1}\right)^2 + \frac{1}{2}\frac{\partial \sigma_s}{\partial \sqrt{J_2'}}\right)^2}\right]^{\frac{1}{2}} \tag{13}$$

Substitution of Equation 11 into Equation 13 yields

$$\gamma g\left(\frac{\sigma_s}{B}\right) = \left[\frac{\frac{1}{3}\left(\frac{d\varepsilon_{kk}^{vp}}{dt}\right)^2 + 2\left(\frac{d\bar{e}^{vp}}{dt}\right)^2}{3\left(\frac{\partial \sigma_s}{\partial J_1}\right)^2 + \frac{1}{2}\left(\frac{\partial \sigma_s}{\partial \sqrt{J_2'}}\right)^2}\right]^{\frac{1}{2}} \tag{14}$$

where

$$\frac{d\bar{e}^{vp}}{dt} = \left[\frac{1}{2}\frac{de_{ij}^{vp}}{dt}\frac{de_{ij}^{vp}}{dt}\right]^{\frac{1}{2}} = \text{square root of the second invariant of the viscoplastic strain rate deviation tensor}$$

Inverting Equation 14 results in

$$\frac{\sigma_s}{B} - g^{-1}\left\{\frac{1}{\gamma}\left[\frac{\frac{1}{3}\left(\frac{d\varepsilon_{kk}^{vp}}{dt}\right)^2 + 2\left(\frac{d\bar{e}^{vp}}{dt}\right)^2}{3\left(\frac{\partial \sigma_s}{\partial J_1}\right)^2 + \frac{1}{2}\left(\frac{\partial \sigma_s}{\partial \sqrt{J_2'}}\right)^2}\right]^{\frac{1}{2}}\right\} = 0 \tag{15}$$

Comparison of Equation 7 with Equation 15 yields the following expression for the parameter β/B

$$\frac{\beta}{B} = g^{-1}\left\{\frac{1}{\gamma}\left[\frac{\frac{1}{3}\left(\frac{d\epsilon_{kk}^{vp}}{dt}\right)^2 + 2\left(\frac{d\bar{e}^{vp}}{dt}\right)^2}{3\left(\frac{\partial \sigma_s}{\partial J_1}\right)^2 + \frac{1}{2}\left(\frac{\partial \sigma_s}{\partial \sqrt{J_2'}}\right)^2}\right]^{\frac{1}{2}}\right\} \tag{16}$$

Equation 16 implicitly represents the dependence of the dynamic yield surface on the viscoplastic strain rate tensor.

Total Strain Rate Tensor

10. The total strain rate tensor can be obtained by combining Equations 3 and 9; thus,

$$\frac{d\epsilon_{ij}}{dt} = \frac{1}{9K}\frac{dJ_1}{dt}\delta_{ij} + \frac{1}{2G}\frac{dS_{ij}}{dt} + \gamma g\left(\frac{\sigma_s}{B}\right)\left[\frac{\partial \sigma_s}{\partial J_1}\delta_{ij} + \frac{1}{2\sqrt{J_2'}}\frac{\partial \sigma_s}{\partial \sqrt{J_2'}}S_{ij}\right] \tag{17}$$

Similarly, the stress rate tensor can be written as

$$\frac{d\sigma_{ij}}{dt} = K\frac{d\epsilon_{kk}}{dt}\delta_{ij} + 2G\frac{de_{ij}}{dt} - \gamma g\left(\frac{\sigma_s}{B}\right)\left[3K\frac{\partial \sigma_s}{\partial J_1}\delta_{ij} + G\frac{\partial \sigma_s}{\partial \sqrt{J_2'}}\frac{S_{ij}}{\sqrt{J_2'}}\right] \tag{18}$$

Equation 17 or 18 is the general constitutive equation for an elastic-viscoplastic isotropic material. To use these equations, it is only necessary to specify the functional forms of K, G, σ_s, and $g(\sigma_s/B)$ and to determine experimentally the numerical values of γ and the coefficients in these functions. The development of a specific elastic-viscoplastic constitutive model for earth materials is presented in the following section.

PART III: ELASTIC-VISCOPLASTIC MODEL FOR EARTH MATERIALS

11. Before the development of the elastic-viscoplastic model is described, it may be useful to briefly discuss some of the salient features of the stress-strain properties of soil under dynamic loading. In the case of most soils, the strength of the material increases with increasing rate of deformation. Because of this dependency on the rate of deformation, the overall character of the dynamic stress-strain curves often differs considerably from that of the corresponding curves obtained under static loading conditions (Whitman, 1970).

12. Figure 4 depicts qualitatively typical stress-strain relations under axisymmetric triaxial test conditions for various rates of strain. As indicated in Figure 4, the soil specimens are hydrostatically consolidated to the same confining pressure (point 1, Figure 4). The samples are then sheared at different rates of strain by increasing the vertical stress σ_z while the radial stress σ_r is held constant. The important behavior to be observed from Figure 4 is that, as the rate of strain $d\varepsilon_z/dt$ increases, the strength of the material also increases. Therefore, associated with each strain rate, the material possesses a unique failure envelope which may be referred to as "dynamic failure envelope." The implications of the dynamic failure envelope can best be realized from the results of a variable strain rate test.

13. It is possible for a material that strain hardens under static loading conditions to exhibit strain-softening behavior due to strain rate effects during dynamic loading. For example, Figure 5 depicts the hypothetical result of such a test superimposed on the corresponding result from a static test. Similar to Figure 4, the two stress-strain relations in Figure 5 are associated with axisymmetric triaxial tests and are hydrostatically consolidated to the same confining pressure. In the case of the dynamic test, the strain rate during the initial part of the test (point 1 to point 2 in Figure 5) is increasing. Beyond point 2, the strain rate decreases. During the initial part of the test, the strength of the material continuously

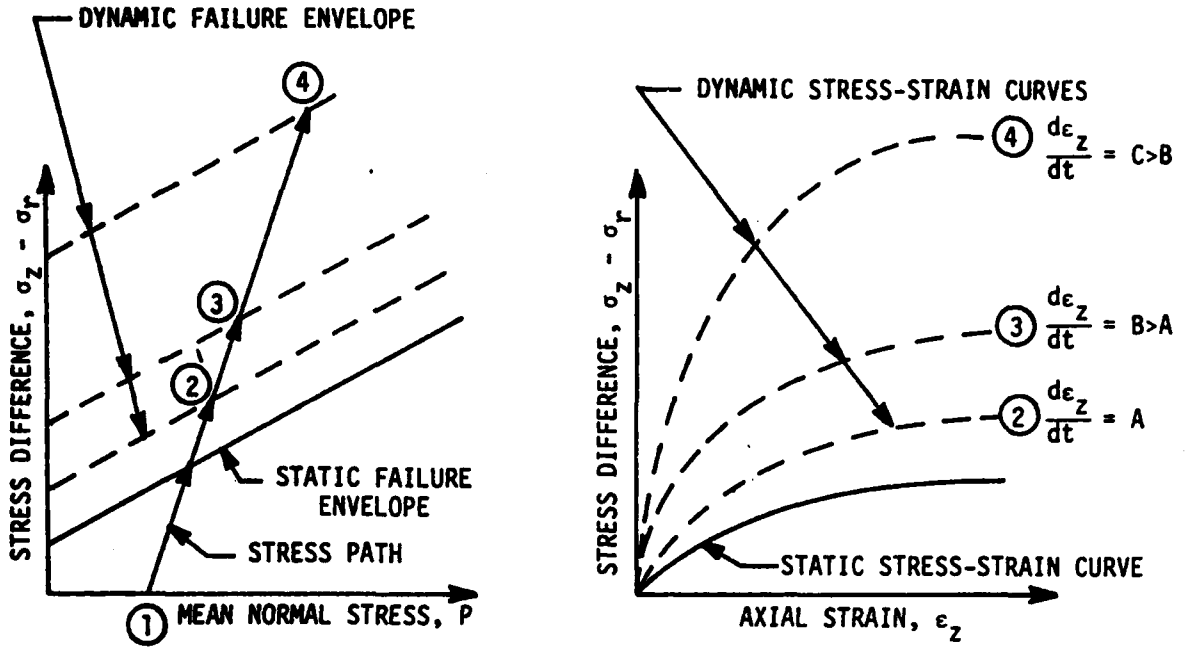

Figure 4. Typical stress-strain curves for different strain rates from an axisymmetric triaxial test

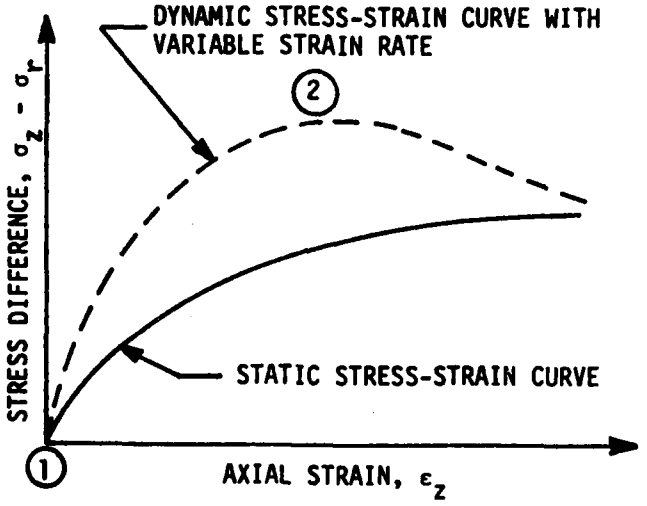

Figure 5. Dynamic stress-strain curve for a variable strain rate from an axisymmetric triaxial test

increases because of the increasing strain rate. Beyond point 2, the strength of the material actually decreases because of the decreasing strain rate, resulting in a "falling" or softening stress-strain curve.

14. In the following section, the mathematical forms of the various response functions are developed for a proposed constitutive model for earth materials.

Elastic Response Functions

15. The behavior of the model in the elastic (recoverable) range is described by the elastic bulk and shear moduli. The elastic bulk modulus is assumed to be a function of the first invariant of the stress tensor J_1 (Figure 6). The elastic shear modulus, on the other hand, is assumed to be a function of the second invariant of the stress deviation tensor J_2' (Figure 7), i.e.,

$$K = \frac{K_i}{1 - K_1} \left[1 - K_1 \exp(-K_2 J_1)\right] \tag{19}$$

$$G = \frac{G_i}{1 - G_1} \left[1 - G_1 \exp(-G_2 \sqrt{J_2'})\right] \tag{20}$$

where

K_i = initial elastic bulk modulus

K_1 and K_2 = material constants

G_i = initial elastic shear modulus

G_1 and G_2 = material constants

The constants K_i, K_1, and K_2 can be determined from the characteristics of the unloading curve from an isotropic consolidation test (Figure 8). The constants G_i, G_1, and G_2 can be determined from the

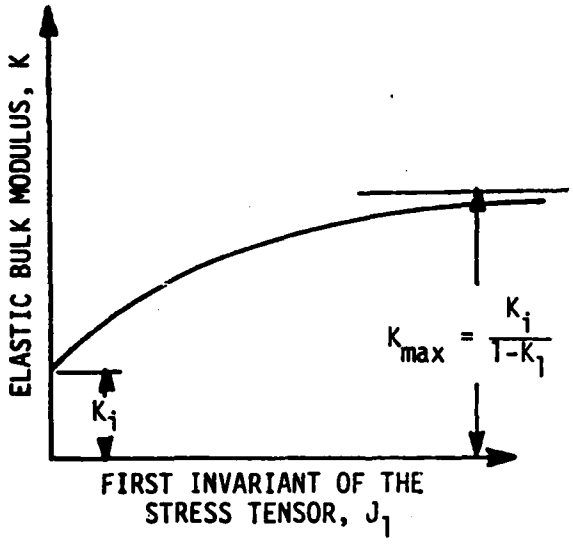

Figure 6. Elastic bulk modulus versus first invariant of the stress tensor

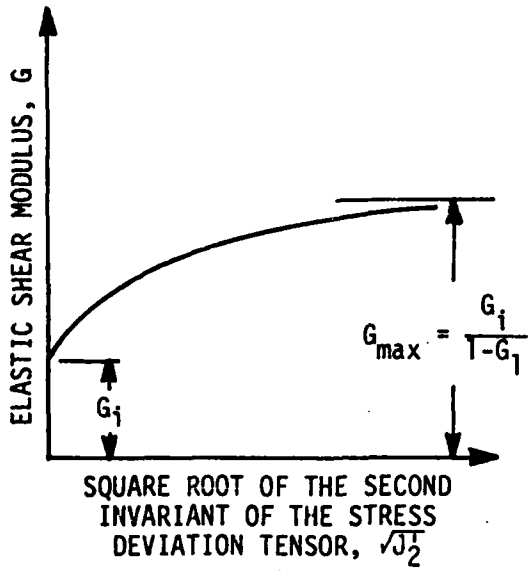

Figure 7. Elastic shear modulus versus second invariant of the stress deviation tensor

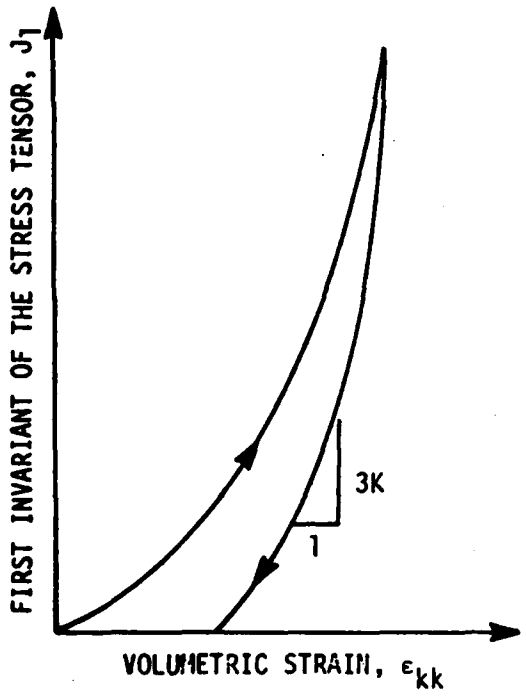

Figure 8. Proposed relationship for isotropic compression test

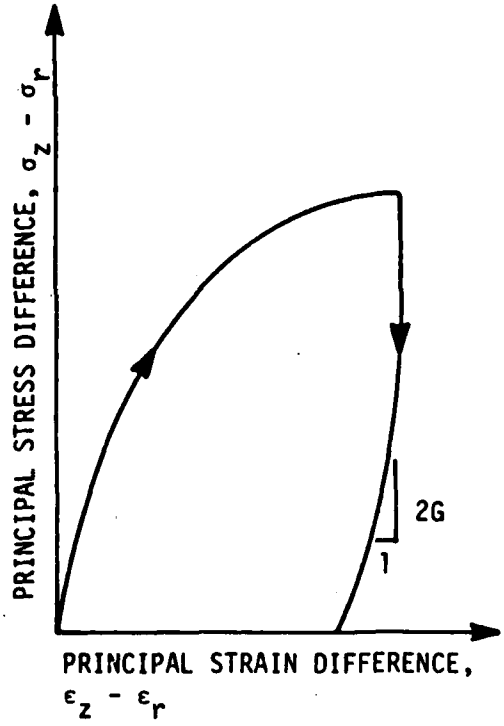

Figure 9. Proposed relationship for triaxial shear test

characteristics of the unloading stress difference-strain difference curves from triaxial shear tests (Figure 9).

Viscoplastic Behavior

16. For the plastic behavior, the dynamic loading function f_d (Equation 7) is assumed to be isotropic and to consist of two parts (Figure 10): a rate-dependent ultimate failure envelope and a rate-dependent strain-hardening yield surface. The failure envelope portion of the loading function is assumed to be of the Prager-Drucker type and is denoted by

$$f_d(J_1, \sqrt{J_2'}, \beta) = \frac{f_s(J_1, \sqrt{J_2'}) - \beta}{B} = \frac{\sqrt{J_2'} - \alpha J_1 - k - \beta}{B} = 0 \qquad (21)$$

and the rate-dependent strain-hardening yield surface is assumed to be elliptical and of the following form

$$F_d(J_1, \sqrt{J_2'}, \kappa, \beta) = \frac{F_s(J_1, \sqrt{J_2'}, \kappa) - \beta}{B} = \frac{\sqrt{(J_1 - L)^2/R^2 + J_2'} - (\kappa - L)/R - \beta}{B} = 0 \qquad (22)$$

The parameters k and α in Equation 21 are material constants representing the static cohesive and frictional strength of the material, respectively. The parameter R (Equation 23 below) in Equation 22 is the ratio of the major to the minor axes of the elliptic yield surface (Figure 10). L and $\kappa + \beta$ in Figure 10 define the intersections of each elliptical yield surface (Equation 22) with the failure envelope $f_d(J_1, \sqrt{J_2'}, \beta)$ and the J_1 axis, respectively. The hardening parameter κ is generally a function of the history of the viscoplastic strain. For the present model, R and κ are chosen to be

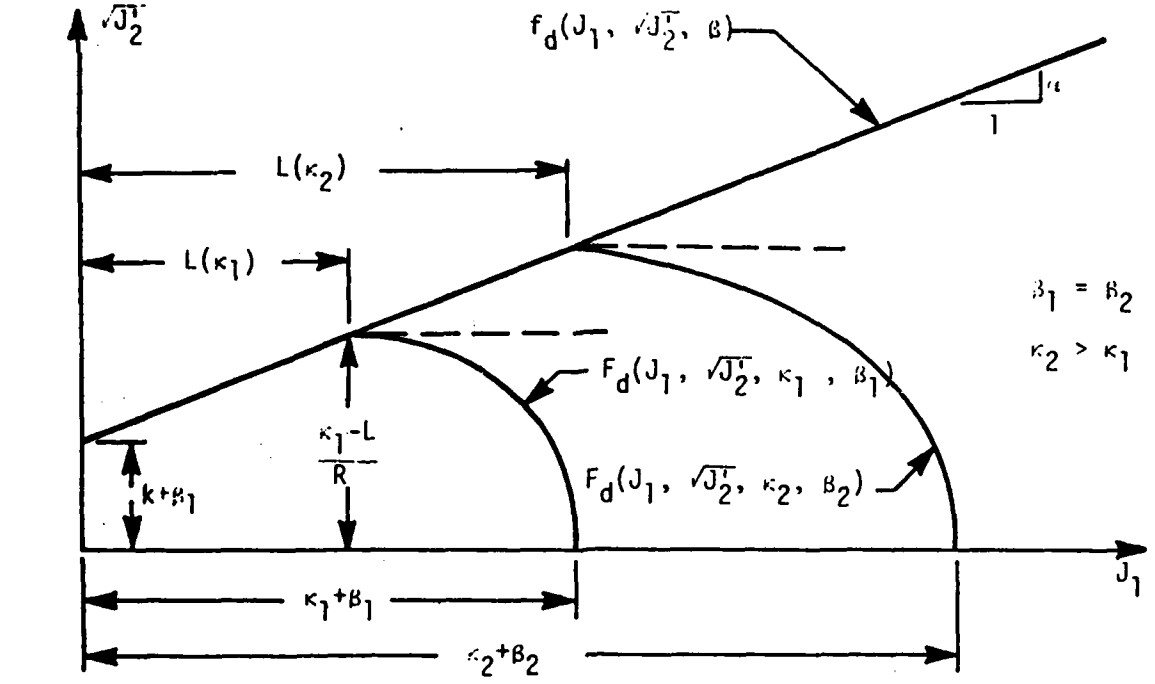

a. Strain-hardening yield surface

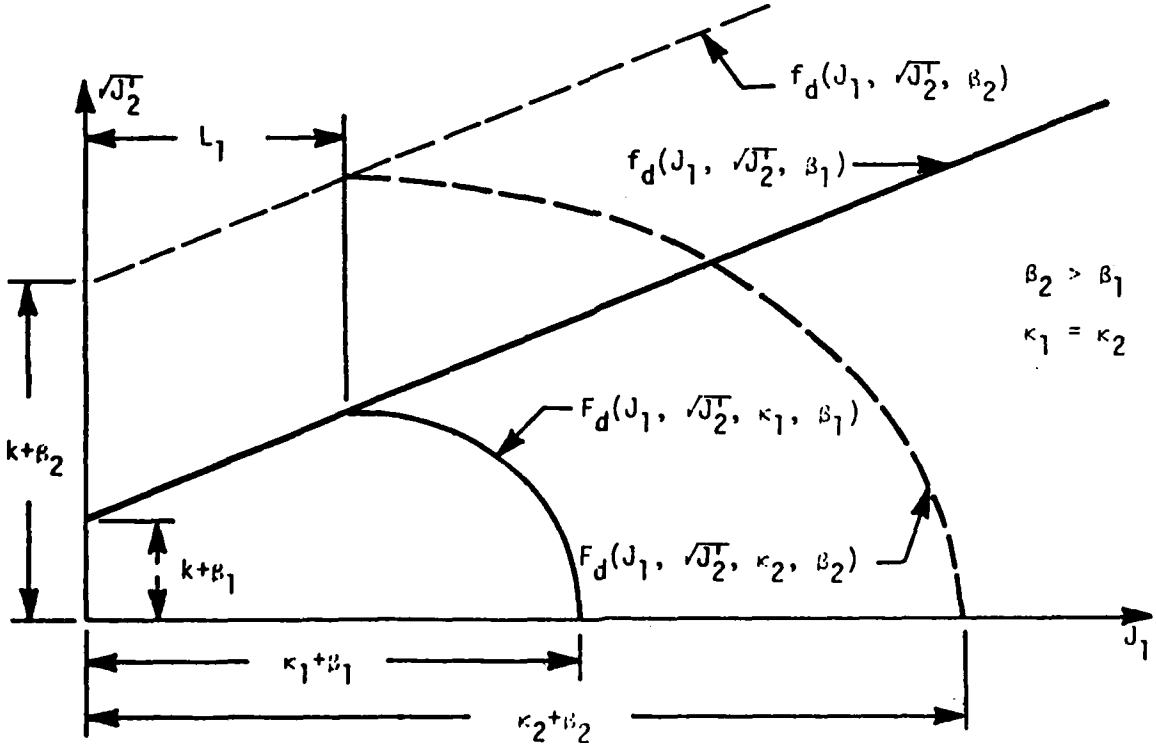

b. Rate-dependent yield surface

Figure 10. Proposed yield surface for the elastic-viscoplastic model

$$R = \frac{R_o}{1 + R_1} \left[1 + R_1 \exp(-R_2 L)\right] \tag{23}$$

$$\kappa = -\frac{1}{D} \ln\left(1 - \frac{\varepsilon_{kk}^{vp}}{W}\right) \tag{24}$$

where R_o , R_1 , R_2 , D , and W are material constants.

17. In order to complete the specification of the model in the viscoplastic range, the function $g(f_s/B)$ (see Equation 8) must be specified. For the present model, $g(f_s/B)$ is chosen to be

$$\left.\begin{aligned} g\left(\frac{f_s}{B}\right) &= \exp\left(\frac{B_1 f_s}{B}\right) - 1 \quad \text{on the failure envelope} \\ g\left(\frac{F_s}{B}\right) &= \exp\left(\frac{B_1 F_s}{B}\right) - 1 \quad \text{on the hardening surface} \end{aligned}\right\} \tag{25}$$

in which B_1 is a material constant controlling the rate of change in the value of the function g . Note in Figure 10 that the elliptic yield surface has a horizontal tangent at its intersection with the failure envelope. This can be assured by the following relation:

$$L = \frac{\kappa - Rk}{1 + \alpha R} \tag{26}$$

In summary, the proposed model contains 16 material constants. Six of the constants (K_i , K_1 , K_2 , G_i , G_1 , and G_2) are related to the elastic response of the material, and the remaining 10 constants (B , B_1 , α , k , R_o , R_1 , R_2 , D , W , and γ) describe the material's viscoplastic response. The behavior of the proposed model under conventional laboratory test conditions (cylindrical specimens) is examined in the following section.

PART IV: BEHAVIOR OF THE MODEL UNDER A CYLINDRICAL STATE OF STRESS

18. The rate-dependent nature of the proposed model can be demonstrated by examining the behavior of the model under particular laboratory test boundary conditions. Since most mechanical testing of soils for engineering purposes is performed with the standard triaxial shear test apparatus, it is useful to investigate the behavior of the model in cylindrical coordinates. Adopting the z-axis of a cylindrical coordinate system (z , r , and θ) as the axis of symmetry of the sample, the stress tensor and the strain tensor associated with this configuration become

$$\sigma_{ij} = \begin{bmatrix} \sigma_z & 0 & 0 \\ 0 & \sigma_r & 0 \\ 0 & 0 & \sigma_r \end{bmatrix} \tag{27}$$

and

$$\varepsilon_{ij} = \begin{bmatrix} \varepsilon_z & 0 & 0 \\ 0 & \varepsilon_r & 0 \\ 0 & 0 & \varepsilon_r \end{bmatrix} \tag{28}$$

The variables $P = J_1/3$ (mean normal stress), J_2' (the second invariant of the stress deviation tensor), and $\varepsilon_{kk}/3$ (mean volumetric strain) associated with the above stress and strain tensors take the following forms

$$P = \frac{J_1}{3} = \frac{\sigma_z + 2\sigma_r}{3} \tag{29}$$

$$J_2' = \frac{(\sigma_z - \sigma_2)^2}{3} \tag{30}$$

$$\frac{\varepsilon_{kk}}{3} = \frac{\varepsilon_z + 2\varepsilon_r}{3} \tag{31}$$

Generally, every triaxial test has two phases: the hydrostatic phase and the shear phase. These phases are discussed below.

Hydrostatic Phase

19. During the hydrostatic phase of the triaxial test, all stresses and strains are equal. Thus,

$$\sigma_z = \sigma_r = J_1/3 = P \tag{32}$$

$$\varepsilon_z = \varepsilon_r = \frac{\varepsilon_{kk}}{3} \tag{33}$$

The relationship between the elastic volumetric strain rate and the rate of the first invariant of stress is given as (Equation 3)

$$\frac{dJ_1}{dt} = 3K\frac{d\varepsilon^E_{kk}}{dt} \tag{34}$$

in which the elastic bulk modulus K is given in Equation 19. Substituting Equation 19 in Equation 34 and integrating the resulting expression provides the following relation between the elastic volumetric strain and the first invariant of the stress tensor:

$$\varepsilon^E_{kk} = \frac{1 - K_1}{3K_2K_i} \ln\left[\frac{\exp(K_2J_1) - K_1}{1 - K_1}\right] \tag{35}$$

The function β/B (Equation 16) for the hydrostatic phase takes the following form:

$$\frac{\beta}{B} = g^{-1}\left\{\frac{\frac{1}{\gamma\sqrt{3}}\left|\frac{d\varepsilon_{kk}^{vp}}{dt}\right|}{\left[3\left(\frac{\partial F_s}{\partial J_1}\right)^2 + \frac{1}{2}\left(\frac{\partial F_s}{\partial \sqrt{J_2'}}\right)^2\right]^{\frac{1}{2}}}\right\} \tag{36}$$

In view of Equations 22 and 25, Equation 36 results in

$$\frac{d\varepsilon_{kk}^{vp}}{dt} = \frac{3\gamma}{R}\left\{\exp\left[\frac{B_1(J_1 - \kappa)}{RB}\right] - 1\right\} \tag{37}$$

Substitution of Equation 24 into Equation 37 yields

$$\frac{d\varepsilon_{kk}^{vp}}{dt} = \frac{3\gamma}{R}\left\{\exp\left[\frac{B_1 J_1}{RB} + \frac{B_1}{BDR}\,\ell n\left(1 - \frac{\varepsilon_{kk}^{vp}}{W}\right)\right] - 1\right\} \tag{38}$$

For a specified rate of loading, Equation 38 can be integrated to yield a relationship between viscoplastic volumetric strain and time. For the same specified rate of loading, the elastic volumetric strain-time response can be calculated from Equation 35. The total volumetric strain-time response can then be determined by adding the viscoplastic strain calculated from Equation 38 and the elastic strain obtained from Equation 35.

20. Note in Equation 38 that when $\gamma = \infty$ (i.e., for an inviscid plastic material) Equation 38 results in

$$\exp\left[\frac{B_1 J_1}{RB} + \frac{B_1}{BDR}\,\ell n\left(1 - \frac{\varepsilon_{kk}^{vp}}{W}\right)\right] - 1 = 0 \tag{39}$$

or

$$\varepsilon_{kk}^{vp} = W[1 - \exp(-DJ_1)] \tag{40}$$

As a result of Equations 35 and 40, the total volumetric strain for inviscid elastic-plastic materials takes the following form:

$$\varepsilon_{kk} = \frac{1 - K_1}{3K_2K_1} \ln\left[\frac{\exp(K_2J_1) - K_1}{1 - K_1}\right] + W[1 - \exp(-DJ_1)] \tag{41}$$

As expected, the volumetric strain in Equation 41 is independent of the time rate of applied loading.

Shear Phase

21. For the shear phase, a constant mean normal stress test will be considered. For this stress path,

$$\frac{dJ_1}{dt} = 0 \tag{42}$$

$$\frac{d\varepsilon_{kk}}{dt} = \begin{cases} 0 \text{ in the elastic range} \\ \dfrac{d\varepsilon^{vp}_{kk}}{dt} \text{ in the viscoplastic range} \end{cases} \tag{43}$$

$$\frac{d\varepsilon^{E}_{kk}}{dt} = 0 \tag{44}$$

The relationship between the elastic strain deviation rate tensor and the rate of stress deviation tensor is given as (Equation 3)

$$\frac{de^{E}_{ij}}{dt} = \frac{1}{2G}\frac{dS_{ij}}{dt} \tag{45}$$

where the elastic shear modulus G is given in Equation 20. The function β/B (Equation 16) takes the following form:

$$\frac{\beta}{B} = g^{-1}\left\{\frac{1}{\gamma}\left[\frac{\frac{1}{3}\left(\frac{d\varepsilon_{kk}^{vp}}{dt}\right)^2 + 2\left(\frac{d\bar{e}^{vp}}{dt}\right)^2}{3\left(\frac{\partial F_s}{\partial J_1}\right)^2 + \frac{1}{2}\left(\frac{\partial F_s}{\partial \sqrt{J_2'}}\right)^2}\right]^{\frac{1}{2}}\right\}, \tag{46}$$

In view of Equations 12 and 22, Equation 46 can be rewritten in the following form:

$$g\left(\frac{F_s}{B}\right) = \frac{1}{\gamma}\left[\frac{\frac{1}{3}\left(\frac{d\varepsilon_{kk}^{vp}}{dt}\right)^2 + \frac{1}{2}\gamma^2\left[g\left(\frac{F_s}{B}\right)\right]^2 \frac{J_2'}{(J_1 - L)^2/R^2 + J_2'}}{\frac{3(J_1 - L)^2/R^4 + \frac{1}{2}J_2'}{\frac{(J_1 - L)^2}{R^2} + J_2'}}\right]^{\frac{1}{2}} \tag{47}$$

Equation 47, in conjunction with Equation 25, leads to

$$\frac{d\varepsilon_{kk}^{vp}}{dt} = \frac{3(J_1 - L)/R^2}{\sqrt{(J_1 - L)^2/R^2 + J_2'}}\gamma\left\{\exp\left[\frac{B_1\sqrt{(J_1 - L)^2/R^2 + J_2'} - B_1(\kappa - L)/R}{B}\right] - 1\right\} \tag{48}$$

Equation 48 describes the coupling between the volumetric strain and the shear stress (J_2' in this case) during a constant mean normal stress test. For a specified time history of J_2', Equation 48 can be integrated to determine the resulting time history of the viscoplastic volumetric strain. From Equations 12, 22, and 25, the following expression is obtained for the viscoplastic strain deviation rate tensor:

$$\frac{de_{ij}^{vp}}{dt} = \frac{1}{2} \frac{\gamma S_{ij}}{\sqrt{(J_1 - L)^2/R^2 + J_2'}} \left\{ \exp\left[\frac{B_1 \sqrt{(J_1 - L)^2/R^2 + J_2'} - B_1(\kappa - L)/R}{B} \right] - 1 \right\} \tag{49}$$

Equations 45 through 49 provide a complete specification for the behavior of the material for constant mean normal stress triaxial tests. These equations, however, must be integrated numerically in order to relate stresses to strains during dynamic loading. A computer program has been developed for numerical integration of the governing equations of the proposed model for general three-dimensional states of stress. For the sake of brevity, the numerical implementation of the model is not described herein. In the following section, the behavior of the model is correlated with test data for a clayey sand using this computer program.

PART V: CORRELATION OF TEST DATA WITH MODEL BEHAVIOR

22. In this section, the behavior of the model under states of uniaxial strain and triaxial shear are correlated with available test data for a clayey sand classified as SC according to the Unified Soil Classification System. Static data consisted of (a) load-unload axial stress-axial strain relations (σ_z versus ε_z) for uniaxial strain, and the corresponding stress paths expressed in terms of principal stress difference versus mean normal stress ($\sigma_z - \sigma_r$ versus P), and (b) two triaxial shear test load-unload stress-strain relations (for two different confining stresses) presented in terms of principal stress difference versus principal strain difference ($\sigma_z - \sigma_r$ versus $\varepsilon_z - \varepsilon_r$), and a static failure envelope based on these two tests (Ehrgott, 1978). The available dynamic data for this material consisted of several stress-strain curves from dynamic uniaxial strain tests (Jackson, Ehrgott, and Rohani; 1980).

23. The first step in correlating the behavior of the model with test data is to simulate the static properties of the material and to determine the numerical values of the material constants K_i, K_1, K_2, G_i, G_1, G_2, α, k, R_o, R_1, R_2, D, and W. The response of the material under static loading is governed by these constants (i.e., the case of inviscid plasticity when rate dependency is neglected). Figure 11 portrays the static test data and the corresponding model behavior for both the triaxial shear and the uniaxial strain test conditions. It can be noted from Figure 11 that the model has reasonably simulated the static response of the soil both qualitatively (triaxial shear response) and quantitatively (uniaxial strain response). The next step is to simulate the available dynamic stress-strain properties of the material, using the numerical values of the 13 constants above and numerical values determined for the remaining three constants B, B_1, and γ. As indicated before, the available dynamic data for this material are limited to several uniaxial strain stress-strain relations. The dynamic data were obtained for loading

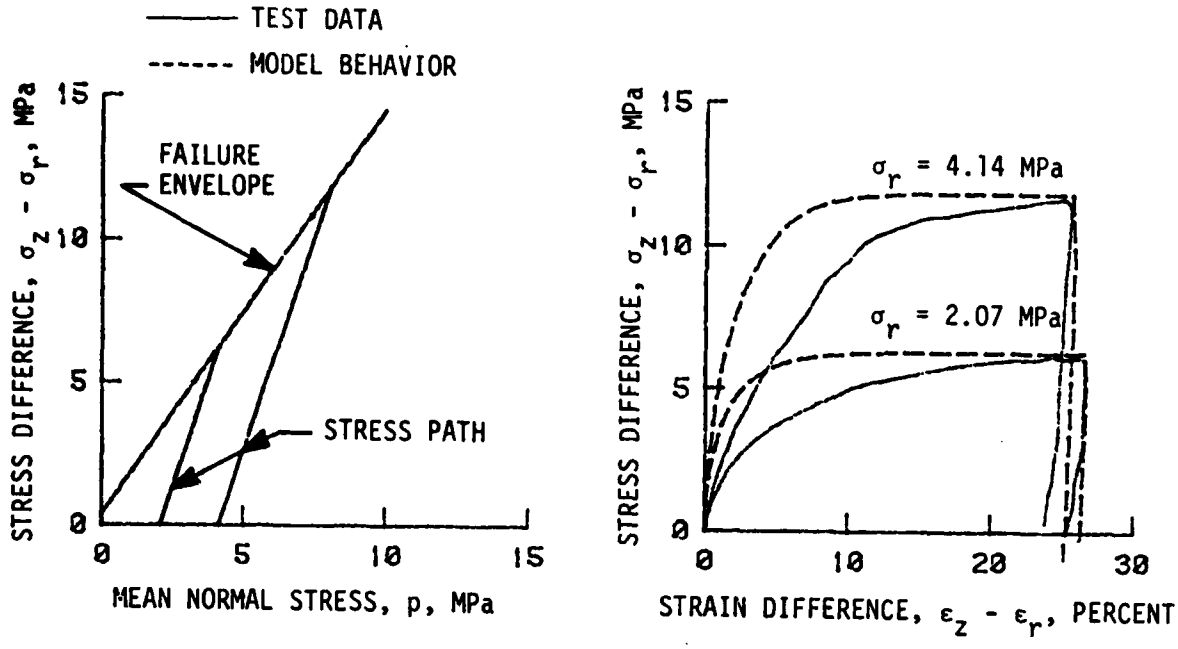

a. Triaxial shear response

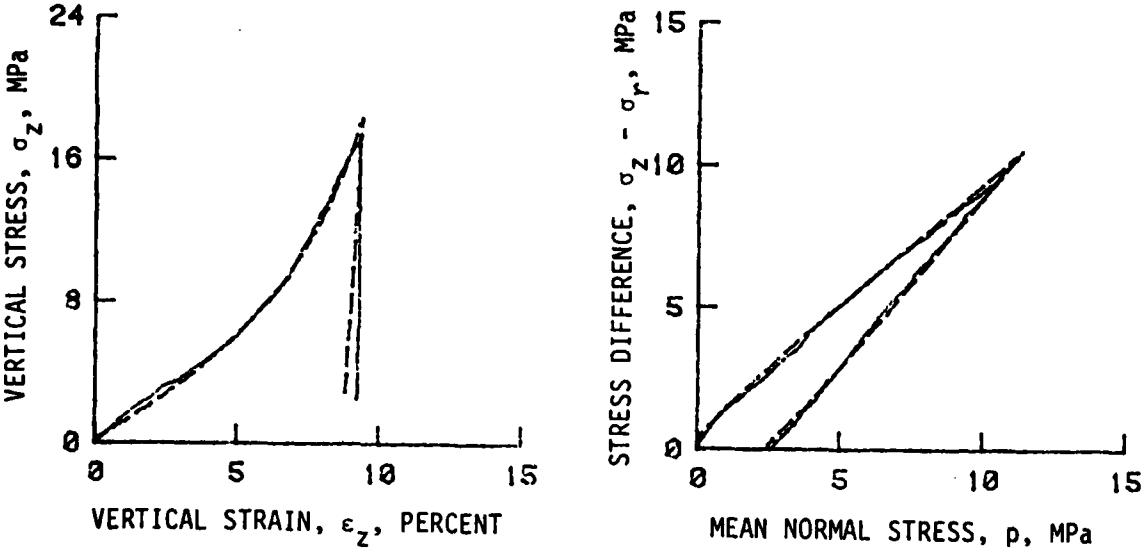

b. Uniaxial strain response

Figure 11. Static response of the material in triaxial shear and uniaxial strain tests; model behavior versus test results

rise times on the order of a few tenths of a millisecond (Jackson, Ehrgott, and Rohani; 1980). Two of the dynamic stress-strain curves were used for the purpose of model fitting. Figure 12a depicts the stress-time histories for the two tests. It should be noted that the entire load-unload cycles for these tests were completed in slightly less than 1 msec. These stress-time histories were used as input for driving the model. The experimental stress-strain curves and the corresponding model behavior for the two dynamic tests are shown in Figure 12b. The agreement between the dynamic test data and the model behavior is very good, both quantitatively and qualitatively, especially during the early part of the test. It is of interest to compare these dynamic stress-strain relations with the corresponding static result in Figure 11b. In the case of the static test, the stress-strain curve is concave to the stress axis (a "stiffening" behavior), whereas the dynamic curves are concave to the strain axis (a "yielding" behavior). The proposed constitutive model predicts this dramatic change in the overall character of the stress-strain curves remarkably well.

24. The numerical values of the 16 material constants for the clayey sand are summarized in Table 1. To demonstrate the application of the proposed model further, the model was driven with the strain-time history shown in Figure 13a under triaxial shear test conditions (σ_r = 2.07 MPa) using the material constants given in Table 1. The resulting dynamic stress-strain curve is shown in Figure 13b. Also shown in Figure 13b is the corresponding static stress-strain curve (from Figure 11a). The effect of the strain rate on the stress-strain response of the material is clearly demonstrated in Figure 13b. As the strain rate increases during the early part of the simulated dynamic test, the stiffness and strength of the material also increases (relative to the static stiffness and strength). During the latter part of the test where strain rate decreases with time, the dynamic curve actually falls (apparent strain softening) and eventually coincides with the static stress-strain curve (at late times).

Table 1

Summary of the Material Constants and Numerical Values for Clayey Sand

Material Constant	Unit of Measure	Numerical Value
K_i	MPa	800
K_1	---	0.5
K_2	MPa^{-1}	0.1
G_i	MPa	480.0
G_1	---	0.5
G_2	MPa^{-1}	0.65
α	---	0.2722
k	MPa	0.231
R_o	---	1.2
R_1	---	-0.5
R_2	MPa^{-1}	0.1
D	MPa^{-1}	0.05
W	---	0.0985
B	MPa	1.0
B_1	---	150,000.0
γ	$msec^{-1}$	0.1

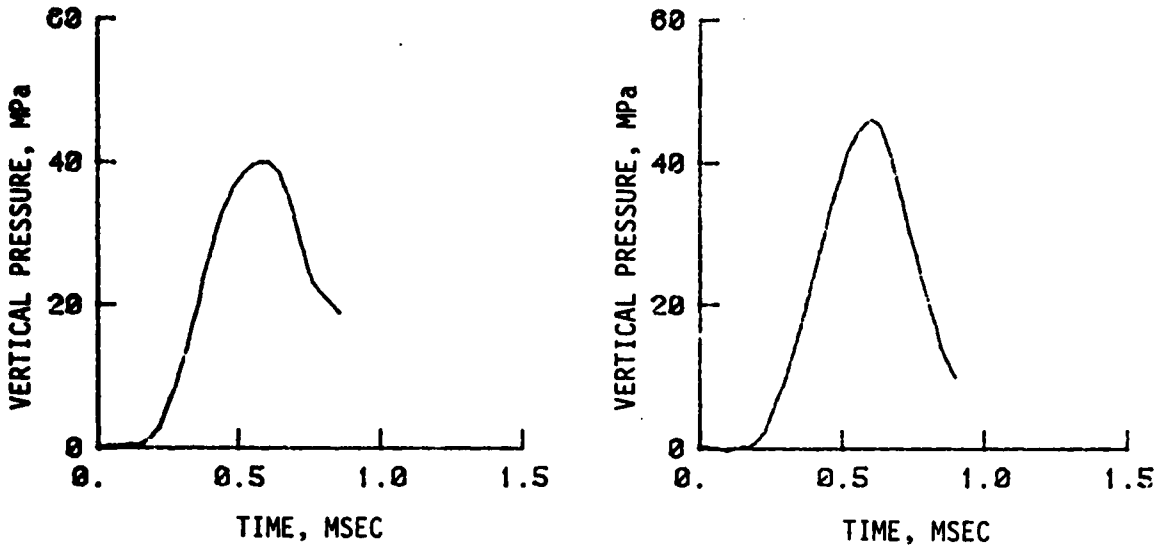

a. Input pressure-time histories

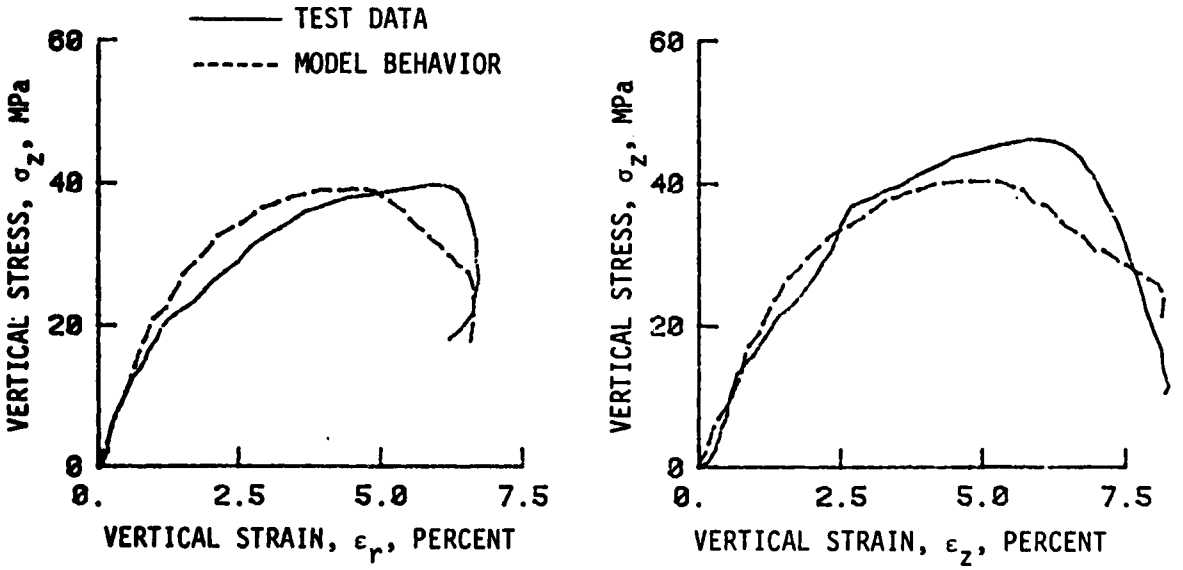

b. Resulting dynamic stress-strain relations

Figure 12. Dynamic response of the material in uniaxial strain configuration; model behavior versus test results

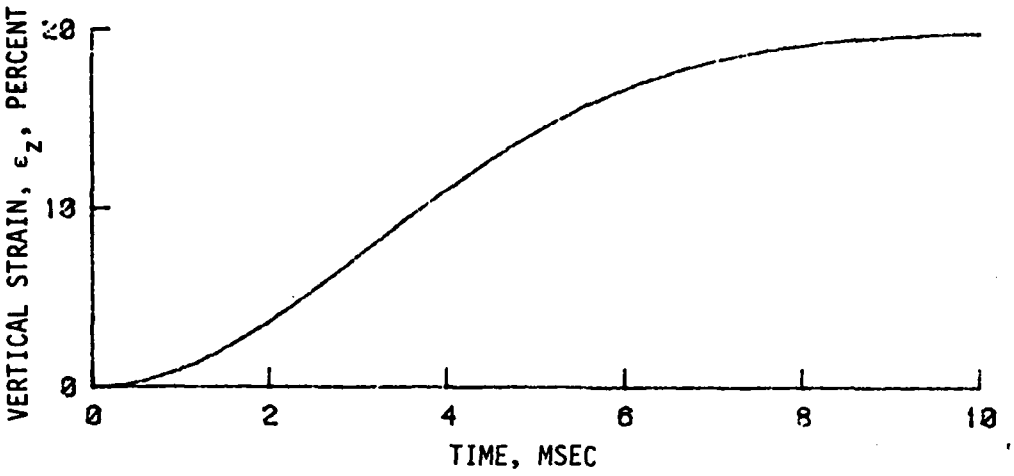

a. Input strain-time history

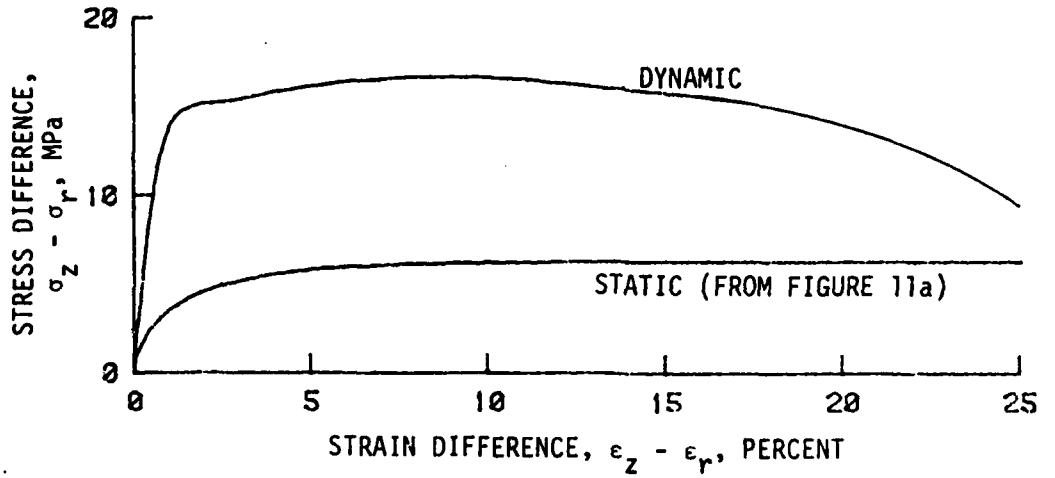

b. Resulting dynamic stress-strain relation

Figure 13. Predicted dynamic stress-strain relation for triaxial shear test condition (σ_r = 2.07 MPa)

PART VI: SUMMARY AND CONCLUSIONS

25. An elastic-viscoplastic constitutive model has been developed for earth materials and has been partially validated via comparison with both static and limited dynamic stress-strain data for a clayey sand. The model is capable of simulating many pertinent features of the stress-strain-strength properties of earth materials such as dependency of the shearing strength of the material on hydrostatic stress and rate of deformation, shear-induced volume change, and permanent deformation under hydrostatic and deviatoric cyclic loadings. In its present form, the model contains 16 material constants that can be readily determined from the results of static and dynamic triaxial shear and uniaxial strain tests.

26. The model has been translated into a numerical algorithm for implementation into finite-difference or finite-element computer codes. The numerical algorithm is very versatile in that it embodies all classes of elastic-plastic constitutive models. Test data for several rates of deformation and test boundary conditions (other than those used to fit the model) are needed to further validate the accuracy and determine the range of application of the model.

REFERENCES

Baladi, G. Y. August 1977. "Numerical Implementation of a Transverse-Isotropic Inelastic, Work-Hardening Constitutive Model," Transactions of the 4th International Conference on Structural Mechanics in Reactor Technology, Vol. M, Methods for Structural Analysis, San Francisco, Calif.

Baladi, G. Y. and Rohani, B. April 1979. "Elastic-Plastic Model for Saturated Sand," Journal of the Geotechnical Engineering Division, ASCE, Vol. 105, No. GT4, Proc. Paper 14510, pp. 465-480.

DiMaggio, F. L. and Sandler, I. October 1971. "The Effect of Strain Rate on the Constitutive Equations of Rocks," Technical Report DNA 2801T, Defense Nuclear Agency, Washington, D. C.

Drucker, D. C. 1956. "On Uniqueness in the Theory of Plasticity," Quarterly of Applied Mathematics, Vol. 14.

Ehrgott, J. Q. 1978. "Loading Response of a Backfill Along Four Different Stress Paths," Internal Data Report, U. S. Army Engineer Waterways Experiment Station, CE, Vicksburg, Miss.

Jackson, J. G., Jr., Ehrgott, J. Q., and Rohani, B. August 1980. "Loading Rate Effects on Compressibility of Sand," Journal of the Geotechnical Engineering Division, ASCE, Vol. 106, No. GT8, Proc. Paper 15640, pp. 839-852.

Perzyna, P. 1966. "Fundamental Problems in Viscoplasticity," Advances in Applied Mechanics, Vol. 9, Academic Press, New York, pp. 243-377.

Sandler, I. S., DiMaggio, F. L., and Baladi, G. Y. July 1976. "Generalized Cap Model for Geological Materials," Journal of the Geotechnical Engineering Division, ASCE, Vol. 102, No. GT7, Proc. Paper 12243, pp. 683-699.

Swift, R. S. July 1975. "Examination of the Mechanical Properties for a Kayenta Sandstone from the MIXED COMPANY Site," Technical Report DNA 3683F, Defense Nuclear Agency, Washington, D. C.

Whitman, R. V. May 1970. "The Response of Soils to Dynamic Loadings; Final Report," Contract Report No. 3-26, Report 26, U. S. Army Engineer Waterways Experiment Station, CE, Vicksburg, Miss.

In accordance with letter from DAEN-RDC, DAEN-ASI dated 22 July 1977, Subject: Facsimile Catalog Cards for Laboratory Technical Publications, a facsimile catalog card in Library of Congress MARC format is reproduced below.

Baladi, George Y.
An elastic-viscoplastic constitutive model for earth materials / by George Y. Baladi and Behzad Rohani (Structures Laboratory, U.S. Army Engineer Waterways Experiment Station). -- Vicksburg, Miss. : The Station ; Springfield, Va. : available from NTIS, 1982.
34 p. : ill. ; 27 cm. -- (Technical report ; SL-82-10)
Cover title.
"December 1982."
Final report.
"Prepared for Office, Chief of Engineers, U.S. Army under Project 4A161102AT22, Task BO, Work Unit 005."
Bibliography: p. 34.

1. Continuum mechanics. 2. Soil mechanics. 3. Soils--Testing. 4. Viscoelasticity. I. Rohani, Behzad. II. United States. Army. Corps of Engineers.

Baladi, George Y.
An elastic-viscoplastic constitutive model for : ... 1982.
(Card 2)

Office of the Chief of Engineers. III. U.S. Army Engineer Waterways Experiment Station. Structures Laboratory. IV. Title V. Series: Technical report (U.S. Army Engineer Waterways Experiment Station) ; SL-82-10.
TA7.W34 no.SL-82-10